Evidence for melting of HD and D$_2$ clusters in solid neon below 1 K

S. Sheludiakov,[*] J. Ahokas, J. Järvinen, L. Lehtonen, and S. Vasiliev
Department of Physics and Astronomy, University of Turku, 20014 Turku, Finland

Yu. A. Dmitriev
Ioffe Institute, 26 Politekhnicheskaya, St. Petersburg 194021, Russian Federation

D. M. Lee and V. V. Khmelenko
*Institute for Quantum Science and Engineering, Department of Physics and Astronomy, Texas A&M University,
College Station, Texas 77843, USA*

We report on an electron spin resonance study of H and D atoms stabilized in solid mixtures of neon, molecular deuterium, and hydrogen deuteride. We observed that H and D atoms can be stabilized in pure HD and D$_2$ clusters formed in pores of solid Ne as well as in a Ne environment. Raising temperature from 0.1 to 1.3 K results in a rapid recombination of a significant fraction of both H and D atoms in HD and D$_2$ clusters. The recombination rate appears to be five and seven orders of magnitude faster than in solid bulk samples of HD and D$_2$, respectively. We explain this recombination rate enhancement by melting of clusters of molecular hydrogen isotopes, similar to what has been observed for atomic hydrogen in H$_2$ clusters [Sheludiakov *et al.*, Phys. Rev. B **97**, 104108 (2018)]. Our observations do not provide evidence for a superfluid behavior of these clusters at temperatures of 0.1–1.3 K.

I. INTRODUCTION

Superfluidity of liquid helium isotopes represents one of the most spectacular macroscopic quantum phenomena. A similar behavior was also predicted for an even lighter spinless bosonic substance, parahydrogen [1]. In contrast to the helium isotopes which remain liquid down to absolute zero, early solidification hinders onset of superfluidity in bulk parahydrogen where supercooling to $T \simeq 1$ K [2,3] is required in order to reach the superfluid transition. Unlike bulk para-H$_2$, small ($N < 30$) molecular hydrogen clusters are expected to remain liquid significantly below the bulk melting temperature ($T_m = 13.8$ K) and exhibit superfluidity [4]. This was eventually confirmed for small ($N \simeq 15$) parahydrogen aggregates in helium nanodroplets at $T \simeq 0.15$ K [5]. The freezing temperature is proportional to the cluster size and may approach zero for very small clusters [6]. The aggregates of a larger size containing $\simeq 10^4$ molecules may still remain liquid at temperature as low as $\simeq 1$ K if prepared in the transient metastable state [6], even though no superfluidity is expected for such clusters in a steady equilibrium state [4,7].

The bulk and cluster-size solids of other molecular hydrogen isotopes, fermionic HD and bosonic D$_2$, are expected to have a similar melting behavior even though smaller zero-point energies should lead to higher freezing temperatures for HD and D$_2$ clusters as compared to those formed from

H$_2$ [8]. Superfluidity was also predicted for small ($N \simeq 10$) clusters of ortho-D$_2$ at temperature about 1 K [9]. The bosonic hydrogen species with a nonzero nuclear spin, such as ortho-H$_2$, have a much lower superfluid transition temperature due to a larger spin-state degeneracy [1].

Small H$_2$ clusters of a nanometer size can be prepared using the gas expansion techniques [10] or stabilization in a highly porous medium with a large specific surface area. Clusters of a greater size can also be prepared by annealing hydrogen films quench condensed onto a cold substrate [11,12]. In our recent study [13], we observed that a large number of such small molecular hydrogen clusters can be accommodated in a porous matrix of quench condensed solid neon films. In addition, an exceptionally high recombination rate of H atoms in such H$_2$ clusters at temperatures 0.3–0.6 K provided evidence for a solid-liquid transition in H$_2$ clusters predicted for solid H$_2$ in a restricted geometry [6].

In this paper, we present a detailed study of the behavior of H and D atoms in Ne matrices containing 1% of HD and ortho-D$_2$, respectively, at temperatures 0.1–1.3 K. We observed the ESR lines of H and D atoms associated with their trapping in clusters of pure HD and D$_2$ formed in solid neon. Similar to a dramatic temperature effect on the ESR lines of H atoms in H$_2$ clusters formed in solid Ne reported earlier [13], we observed a strong enhancement of D and H atom recombination in D$_2$ and HD clusters formed in Ne:1%D$_2$ and Ne:1%HD samples. However, this takes place at temperatures 0.9–1.3 K, slightly higher than that for the Ne:1%H$_2$ solid solution. We also observed that the recombination rates of H and D atoms in clusters of hydrogen isotopes in this temperature range are nearly the same in contrast to a drastic

———————
[*]seshel@physics.tamu.edu; Present address: Institute for Quantum Science and Engineering, Department of Physics and Astronomy, Texas A&M University, College Station, Texas 77843, USA
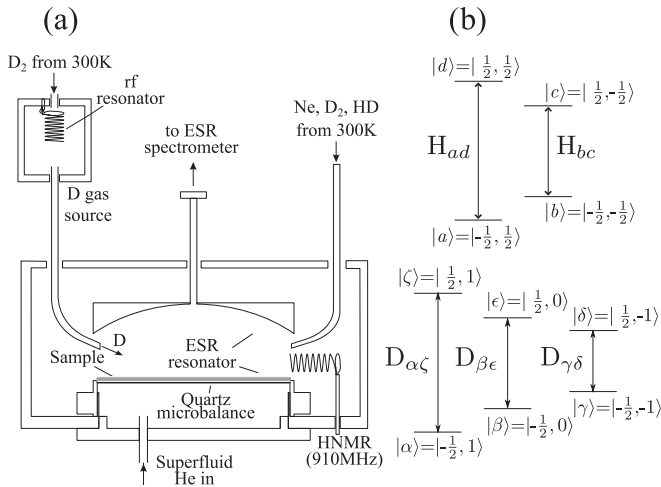
FIG. 1. (a) The sample cell schematic. (b) Energy levels for H (top row) and D atoms (bottom row) in a high magnetic field. The electronic and nuclear spin states are labeled as $|m_S, m_I\rangle$, respectively. The allowed ESR transitions are shown by solid lines.

difference for the bulk solid samples at these temperatures. We suggest that this observation supports our conclusion on melting of molecular hydrogen clusters formed in solid neon made earlier [13]. Based on the similar behavior of H and D atoms in the fermionic HD and bosonic para-H_2 and ortho-D_2 clusters, we conclude that the clusters undergoing a solid-liquid transition are unlikely to be superfluid within the temperature range of our experiment.

II. EXPERIMENTAL SETUP

The experimental setup is based on an Oxford 2000 dilution refrigerator which accommodates a sample cell (SC) [Fig. 1(a)] and a 128 GHz ESR spectrometer [14]. The SC is placed in the center of a 4.6 T superconducting magnet and attached to the mixing chamber of the dilution refrigerator to provide cooling. The main diagnostic tool in our experiments is a 128 GHz heterodyne ESR spectrometer which enables a simultaneous measurement of both absorption and dispersion parts of the mm-wave susceptibility [15]. We will present only the absorption part throughout this paper. The ESR resonator in the sample cell has an open Fabry-Perot design which also allows installation of the lines for condensing neon-molecular hydrogen isotopes gas mixtures and an auxiliary rf resonator [HNMR in Fig. 1(a)]. The top ESR resonator mirror has a spherical shape and is made of oxygen-free polycrystalline copper. The bottom Pd ESR resonator mirror also serves as the top electrode of a quartz microbalance (QM) which makes it possible to measure simultaneously the ESR signals of H and D atoms and determine the film thickness. The energy levels of H and D atoms in a high magnetic field and their allowed ESR transitions are presented in Fig. 1(b). We used neon gas of 99.99% purity which contains 100 ppm natural H_2 admixture. The Ne:D_2 and Ne:HD gas mixtures were prepared at room temperature and the solid films were deposited onto the top electrode of the QM directly from a gas-handling system with a typical rate of 0.1 monolayers/s. The substrate temperature during the film deposition was stabilized

at temperature 0.7–1.3 K. Prior to that, a small amount of He gas($\sim$mmole) was condensed into a chamber below the quartz microbalance in order to form a saturated helium film there. The superfluid film flushes the bottom QM surface and removes heat released during sample deposition. The QM also provides an opportunity to detect possible superfluidity of deposited films which would decouple from the quartz oscillations and lead to an increase of the QM oscillation frequency.

The present sample cell was also used in our previous studies of solid tritium films [16] and, as a result, a number of tritium atoms and molecules remained trapped in the ESR mirrors and the copper walls of the sample cell. The electrons released in β decay of the remaining tritium dissociate a fraction of HD and D_2 molecules in Ne:HD and Ne:D_2 solid samples, respectively, and discernible ESR signals of H and D atoms can be observed after a few hours of sample storage. We utilize this flux of electrons resulting from tritium decay as the main method for dissociation of hydrogen in the deposited films.

Along with the H and D atoms trapped inside solid Ne:HD and Ne:D_2 films, we were also able to create in the sample cell D atoms in the gas phase. The reference ESR lines of D atoms in the gas phase were employed for determining the spectroscopic parameters of the D atoms in Ne:HD and Ne:D_2 samples. A separate chamber, the so-called D-gas source [Fig. 1(a)], was arranged about 5 cm above the sample cell body and a number of D_2 molecules was condensed there in advance [17,18]. The fluxes of D atoms in the gas phase are created by running a rf discharge in the D-gas source. Prior to that, a small, $\simeq 1$ μmole, amount of He gas is condensed into the sample cell in order to initiate the discharge, while the superfluid He film reduces recombination of the gas-phase atoms on the sample cell walls and helps to stabilize a needed quantity of the D atoms in the gas phase.

III. EXPERIMENTAL RESULTS

In the present paper, we extend our previous study of Ne:H_2 mixtures [13] to Ne:1%HD and Ne:1%D_2 solid solutions in order to acquire more information on the melting behavior of clusters of molecular hydrogen isotopes and probe their possible superfluidity. The samples we studied were stored at $T \simeq 90$ mK, the lowest temperature attained in this experimental run, for a time period of several days in order to achieve strong enough ESR signals of H and D atoms (Figs. 2 and 3). Similar to our previous work [13], we observed that the growth rate of H and D atom ESR signals in the Ne:1%D_2 and Ne:1%HD samples significantly exceeded the rate expected based on the D_2 and HD content in the neon matrix. The production rates of H and D atoms in Ne:1%HD and Ne:1%D_2 samples were only a factor of two smaller as compared to a pure H_2 film of the same thickness. However, the accumulation rates of H and D atoms scaled to the estimated number of HD and D_2 molecules in these samples are nearly an order of magnitude greater than that for a pure H_2 sample with no Ne present scaled to the number of H_2 molecules there as presented in Fig. 4. This supports our observations made earlier [13] that a significant number of secondary electrons is generated in the solid neon matrix bombarded by electrons
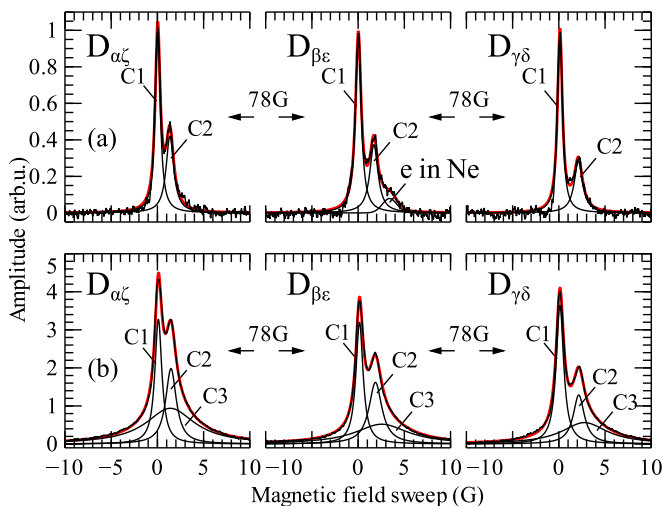
FIG. 2. (a) ESR spectrum of D atoms and trapped electrons in Ne:1%D$_2$ after two days of storage. The electron line appears as a shoulder on Component 2 of D$_{\beta\epsilon}$ line. (b) ESR spectra for the same sample after one week of storage. The electron line becomes concealed by Component 3.

released during the decay of tritium trapped in the sample cell walls. Secondary electrons drastically increase the efficiency for dissociation of D$_2$ and HD molecules in the solid matrix and sufficiently enhance the H and D atom accumulation.

A. ESR spectra of D atoms in Ne:1%D$_2$ sample

The ESR spectrum of D atoms is a triplet of lines separated by 78 G due to hyperfine interaction between electron and nuclear spins. The ESR lines become broadened due to the dipolar interaction of D atom electron spins as well as by their interaction with the nuclear magnetic moments of the host D$_2$ molecules. The former contribution to the line broadening is proportional to the D atom concentration and can be used for determination of their density [21]. In addition to that, the ESR lines of D atoms acquire a composite structure with
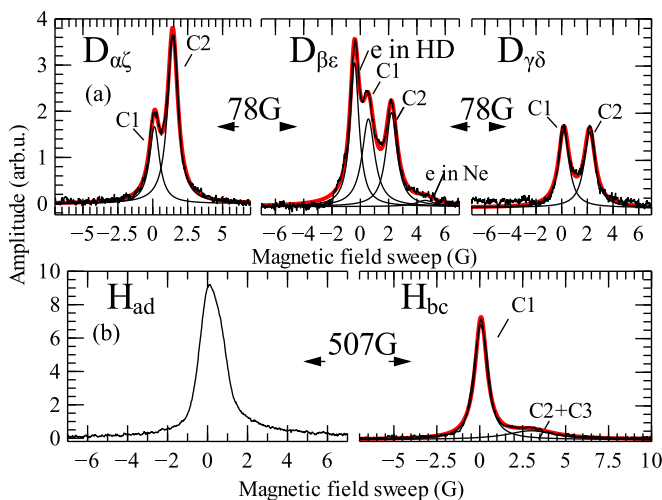

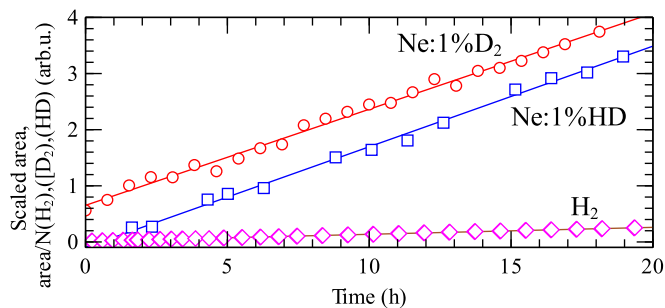FIG. 3. ESR spectra of D (a) and H atoms (b) in the Ne:1%D$_2$ sample.

FIG. 4. Accumulation of H and D atoms in Ne:1%HD (blue squares) and Ne:1%D$_2$ (red circles) samples scaled to the estimated number of HD and D$_2$ molecules in these samples. The accumulation rate of H atoms in a pure 2.5 μm H$_2$ film scaled to the number of H$_2$ molecules there is shown by magenta diamonds for comparison.

several components originating from the D atoms located in different environments: in the clusters of pure D$_2$ and in two different positions in the Ne matrix similar to that observed for the lines of H atoms in the Ne:H$_2$ mixtures [13]. However, in contrast to the Ne:H$_2$ samples, the ESR lines of atomic deuterium in the first two days of storage could be fitted by only two components [Fig. 2(a)].

Unlike D$_{\alpha\zeta}$ and D$_{\gamma\delta}$ lines, the central D$_{\beta\epsilon}$ line of trapped D atoms in this sample possessed a broad shoulder at the high-field side [Fig. 2(a)] which we attributed to trapping electrons in a pure Ne environment similar to that observed in the ESR spectra center of Ne:H$_2$ samples in our previous work [13,22]. The presence of a strong deuterium D$_{\beta\epsilon}$ line in the center of the ESR spectrum [Fig. 2(a)] made it difficult to reliably distinguish a presence of the ESR line of electrons trapped in D$_2$ clusters [22] formed in the Ne:1%D$_2$ sample.

It turned out that an additional broad, ∼6 G wide, component (C3) appeared in the ESR spectra of D atom lines after storing the Ne:D$_2$ sample for three days [Fig. 2(b)]. We carried out the same procedure to determine the spectroscopic parameters for the C3 component as that for C1 and C2 observed in the beginning of storage. The extracted electronic g factor for C3 is $g_{C3} = 2.002195(20)$. Component 3 had a much larger width compared to C1 and C2 which made the determination of its spectroscopic parameters much less accurate. For the same reason we were unable to make a reliable estimate of the hyperfine constant for D atoms corresponding to C3. The spectroscopic parameters for all three components of the D atom ESR lines in this sample are collected in Table I.

B. ESR spectra of H and D atoms in the Ne:1%HD sample

The ESR lines of H and D atoms in the Ne:1%HD sample formed a doublet/triplet separated by 507/78 G, respectively, due to hyperfine interaction of their electron and nuclear spins. ESR lines of both H and D atoms in this sample possessed a complex structure similar to that for H and D in Ne:1%H$_2$ [13] and Ne:1%D$_2$ samples, respectively, which allowed us to conclude that the H and D atoms were stabilized in both pure HD (C1) and pure Ne (C2, C3) environments. We did not observe formation of a broad C3 component for D atom ESR lines in the Ne:1%HD sample as compared to the Ne:1%D$_2$ sample which may also be related to storing this sample for

TABLE I. Spectroscopic parameters and widths of D and H atom ESR line components measured in Ne:1%D_2 and Ne:1%HD samples. Parameters for C1 and C2 components of the D atom ESR line in Ne:1%D_2 film were determined for the fresh sample (1–2 days of storage) and those for C3 after 7 days of sample storage. The parameters of H and D atom ESR line components in Ne:1%HD film were determined after 2 days of storage. We were unable to reliably resolve the structure formed by the C2 and C3 components of H atom ESR lines in Ne:1%HD sample to separate out their contributions to the lineshape.

	g	A (MHz)	$\frac{\Delta A}{A}$ (%)	width (G), fresh	width (G), aged
		D in D_2 clusters (Ne:1%D_2)			
C1	2.002300(10)	218.1(1)	−0.07	0.7	0.9
C2	2.002235(10)	219.2(1)	+0.43%	1.1	1.4
C3	2.002195(20)				6.3
free atoms	2.002284 [19]	218.256 [20]			
		D in HD clusters (Ne:1%HD)			
C1	2.002264(10)			1.0	
C2	2.002225(10)			1.0	
		H in HD cluster (Ne:1%HD)			
C1				0.8	
C2+C3				3.4	

a shorter time than that for the Ne:1%D_2 sample. We were also unable to reliably resolve the structure formed by the C2 and C3 components of the H_{bc} line in the Ne:1%HD sample in order to evaluate their contributions to the observed ESR line envelope. These components merged into a single broad structure on the H_{ad} line where their contributions could not be resolved unambiguously. The ESR spectra of D and H atoms acquired while storing this sample are presented in Fig. 3.

The C1 component of the H atom ESR lines had a stronger amplitude as shown in Fig. 3 as compared to those of the D atoms which provides evidence of ongoing D-H conversion due to the exchange tunneling reaction D+HD → D_2+H taking place in the HD clusters [23]. However, the C2 components of both D and H atom lines had approximately comparable amplitudes as expected for their trapping in the pure Ne environment, where this exchange reaction does not take place. While storing this sample, we were unable to stabilize deuterium and hydrogen atoms in the gas phase and determine the spectroscopic parameters for H and D atoms trapped in the Ne and HD environments. The electronic g factors for the C1 and C2 components of D atom ESR lines for this sample were estimated based on their shifts from the line of electrons trapped in HD clusters formed in solid neon. The g factor of this reference line was considered to be equal to that for electrons trapped in the pure D_2 environment in the Ne:1%D_2 sample. There is no spin-orbit interaction associated with either H and D atoms or molecules of hydrogen isotopes and the g factor of the ESR line of electrons trapped in these different environments should remain the same. Some of the spectroscopic parameters obtained for both H and D atoms in the Ne:1%HD samples are summarized in Table I.

C. Effect of temperature and helium film

In our previous study of H atoms in solid Ne:H_2 mixtures [13] we found that raising temperature from 0.1 to 0.3–0.6 K triggered nearly complete instantaneous recombination of H atoms trapped in H_2 clusters formed in solid neon. This effect turned out to be most pronounced for the Ne:1%H_2 sample

where nearly 60% of these H atoms recombined after raising the SC temperature to 0.6 K. In this work, we carried out a series of experiments to verify the effects of temperature on the ESR line intensities of atomic deuterium and hydrogen in similar solid mixtures in Ne of different hydrogen isotopes, Ne:1%D_2 and Ne:1%HD. The absolute values of atomic concentrations, n, of H and D atoms in the HD and D_2 clusters in solid neon were estimated from the known dependence of the ESR line broadening on concentration [24] and were in the range 5×10^{17}–2×10^{18} cm^{-3} in this work.

Raising the SC temperature from 0.1 to 0.75 K led to an only insignificant, $\simeq$15%, decrease of C1 of the D atom ESR lines in the Ne:1%D_2 sample (Fig. 5). After that, we cooled the cell back to 0.1 K and left the Ne:1%D_2 sample stored at this temperature. It turned out that C1 of the D atom ESR lines continued to grow at the same rate and eventually
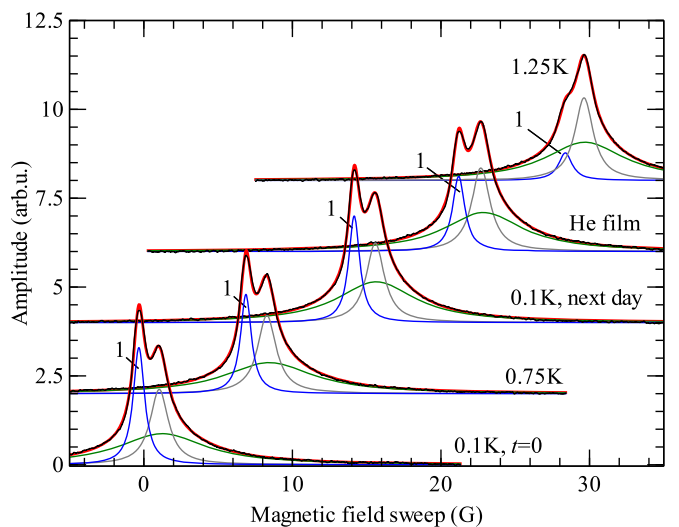
FIG. 5. Effect of temperature and a superfluid helium film on the central $D_{\beta\epsilon}$ ESR lines of D atoms in the Ne:1%D_2 sample. The other ESR lines of D atoms in the Ne:1%D_2 sample behaved identically to the $D_{\beta\epsilon}$ line and are not shown.
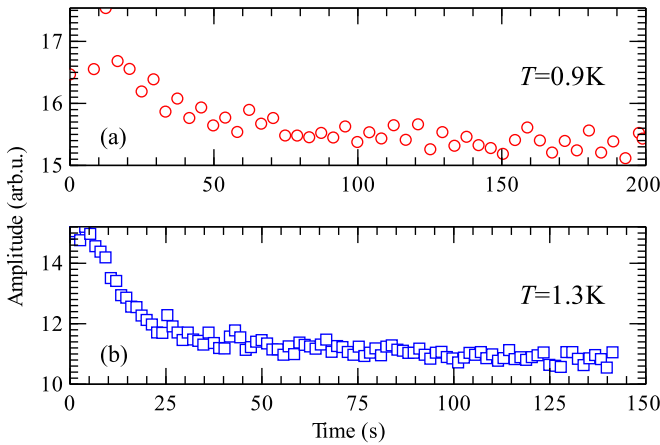
FIG. 6. (a) Time evolution of C1 component amplitude for ESR spectrum of D atoms in Ne:1%D$_2$ sample at $T = 0.9$ and (b) at $T = 1.3$ K. No helium was condensed into the SC.
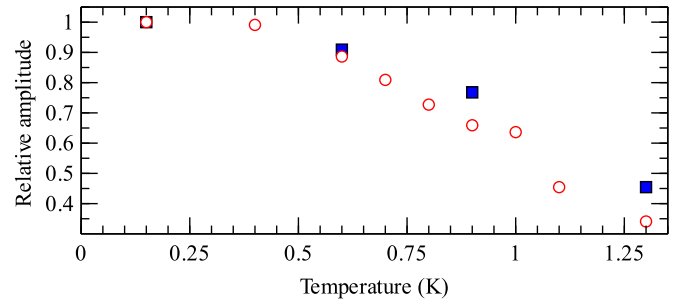

FIG. 7. Normalized amplitudes of the ESR lines of H and D atoms (blue squares and red open circles, respectively) in HD clusters (C1 component) in Ne:1% HD sample. No helium was condensed into the SC.

recovered intensity after one day of storage (Fig. 5). A similar behavior of the H-line C1 was observed previously in the Ne:1%H$_2$ mixture which was recovered after initially raising temperature from 0.1 K to 0.3–0.6 K and subsequent cooling to 0.1 K [13].

At the next stage, we studied the influence of an unsaturated He film on the ESR spectra of D atoms. Component 1 of the D lines in the Ne:1%D$_2$ sample experienced only a modest decrease of about 20% after condensing the He film. However, raising the sample cell temperature further to 1.25 K resulted in a nearly complete, rapid disappearance only of Component 1 in the Ne:1%D$_2$ sample, similar to that observed for the Ne:1%H$_2$ sample after heating from 0.1 K to 0.85 K in the previous work [13]. Evolution of the D atom ESR lines in Ne:1%D$_2$ upon raising the sample cell temperature and condensing the helium film is presented in Fig. 5. The C1 components of the D atom ESR lines did not recover after pumping He from the SC and storing the sample at $T = 0.1$ K for three days.

We also made a separate study aimed at resolving the recombination kinetics of D atoms in D$_2$ clusters at temperatures of 0.9 and 1.3 K *without* condensing He into the SC [Figs. 6(a) and (b)]. The recombination of D atoms at the former temperature was much less efficient and took place with a clearly larger characteristic time. The recombination rate constants, k_r, were estimated assuming the second-order recombination process, $dn/dt = -2k_r n^2$, the half-decay times

found from Fig. 6, and the local concentrations of D atoms in the D$_2$ clusters mentioned earlier.

We were able to estimate the recombination rates of D atoms in D$_2$ clusters in the Ne:1%D$_2$ sample at both temperatures: $k_r = 4(2) \times 10^{-21}$ cm^3 s^{-1} and $7(4) \times 10^{-21}$ cm^3 s^{-1}, for $T = 0.9$ and 1.3 K, respectively. The recombination rates obtained are several orders of magnitude larger than those obtained for D atoms in bulk solid D$_2$ films at these temperatures (Table II). This leads us to the important conclusion that such anomalously high recombination rates of D atoms result from melting of D$_2$ clusters formed in solid neon in accordance to that observed in our previous work for H$_2$ clusters in the solid Ne matrix [13].

Similar results were observed for the Ne:1%HD sample. After the sample had been stored for two days, we started raising the temperature from $T = 0.1$ K in 0.1–0.2 K steps up to 0.9 K. We did not condense He into the sample cell during this study. It turned out that only 20–30% of atoms forming the C1 component of both H and D atoms recombined at this stage (Fig. 7). Raising temperature further, up to 1.3 K led to a rapid, within several seconds, recombination of nearly 50% of H and D atoms forming the C1. The decay of the C1 component of H atom ESR lines as a function of time at $T = 0.9$ and 1.3 K in this sample is shown in Figs. 8(a) and 8(b). The recombination behavior of H and D atoms in HD clusters upon raising temperature turned out to be identical and the H:D ratio of their C1 components almost did not change in the course of this measurement as presented in Fig. 7. The recombination rate constants k_r for H atoms in HD clusters at $T = 0.9$ and 1.3 K were estimated in a manner similar to that described earlier for D atoms in D$_2$ clusters. We were able to estimate the recombination rate constants for

TABLE II. Recombination rates of H and D atom in H$_2$, HD, and D$_2$ clusters formed in solid Ne and solid bulk samples. The calculated rates of exchange reactions H+H$_2 \to$ H$_2$+H, H+HD $\to$ HD+H and D+D$_2 \to$ D$_2$+D are presented for comparison. The recombination and exchange reaction rates are presented in units of cm^3 s^{-1}.

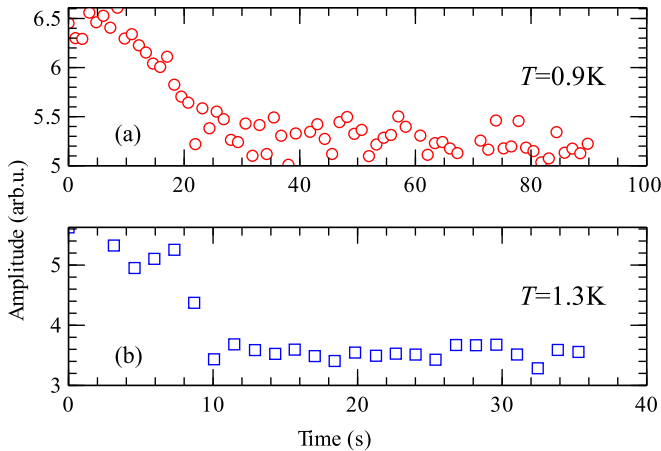| | Clusters in solid Ne | | | | |
	0.6 K	0.9 K	1.3 K	Bulk, $T = 0.9$ K	Exchange reactions at $T = 4.2$ K [25]
H:H$_2$	$5(3) \times 10^{-20}$ [13]			2×10^{-24} [24]	7.6×10^{-25}
H:HD		$5(3) \times 10^{-21}$	$4(2) \times 10^{-20}$	$<3 \times 10^{-25}$	3.5×10^{-27}
D:D$_2$		$4(2) \times 10^{-21}$	$7(4) \times 10^{-21}$	3×10^{-28} [23]	1.2×10^{-30}

FIG. 8. (a) Time evolution of C1 component amplitude for the ESR spectrum of H atoms in Ne:1%HD sample at $T = 0.9$ and (b) at $T = 1.3$ K. No helium was condensed into the SC.

H atoms forming the C1 component at $T = 0.9$ and 1.3 K as $k_r = 5(3) \times 10^{-21}$ cm^3 s^{-1} and $4(2) \times 10^{-20}$ cm^3 s^{-1}, respectively. These recombination rates are much higher than those expected for H and D atoms in bulk HD films at these temperatures (Table II) and are close to those estimated for the D atoms in D$_2$ clusters in the Ne:1%D$_2$ sample. Therefore, we conclude that rapid recombination of H and D atoms forming C1 can also be explained by melting of HD clusters formed in solid Ne.

The recombined fraction of D atoms Ne:1%D$_2$ sample (about 30%) corresponding to C1 is significantly smaller than those of H and D atoms forming C1 in the Ne:1%HD sample (50%) after raising SC temperature to $T = 1.3$ K. This allows us to conclude that a significantly smaller fraction of the D$_2$ clusters melted at $T = 1.3$ K compared to that in the Ne:1%HD solid mixture assuming that the HD and D$_2$ clusters have the same size distribution. We did not observe any reproducible increase of the QM frequency during rapid recombination of the H and D atoms forming C1 in the samples we studied which might have indicated possible superfluidity of melted D$_2$ clusters.

IV. DISCUSSION AND CONCLUSIONS

We observed that D atoms may occupy different sites in the Ne:1%D$_2$ solid mixture corresponding to three ESR line components with a slightly negative (C1) and a clearly positive hyperfine constant change (C2) as compared with the free atom value ($A = 218.256$ MHz [20]). The determination of spectroscopic parameters for the C3 component was less accurate due to the larger linewidth. Component 1 is characterized by the electronic g factor which nearly matches that of the D atoms in bulk D$_2$ samples and may be related to trapping in the pure D$_2$ environment. The g factors of components C2 and C3 are smaller as compared to that of C1 which makes it possible to conclude that these two components correspond to the D atoms trapped in the pure Ne environment. The reduced width of the C1 component, $\simeq 0.7$ G, as compared to that observed for D atoms in pure D$_2$ samples, $\simeq 1.3$ G–2.3 G [26,27], may result from a smaller number, $N < 12$, of the

nearest neighbors which might be expected for the disordered sites in the vicinity of the pore surfaces. Another possibility would be the presence of a certain number of Ne atoms in the vicinity of H and D atoms forming C1. However, this would also decrease the electronic g factor for the D atoms forming C1 due to spin-orbit interaction with the neighboring Ne atoms which was not observed.

In contrast to Components 1 and 2, the broad Component 3 appeared in the ESR spectra of the D atom only after three days of storage. Similar behavior was observed by Sharnoff and Pound who reported on a composite structure of the ESR lines of D atoms embedded in solid D$_2$ [28] produced during β decay of tritium admixed into the deuterium gas before deposition. The ESR lines of atomic deuterium in their study consisted of two components with the widths of 2.2 and 11 G, respectively, and were attributed to atoms occupying similar (substitutional) sites in the D$_2$ lattice. The authors suggested that the larger width of the broader component may be associated with the D atoms produced in the course of dissociation of D$_2$ molecules and thermalized within the distance of a few lattice constants. The larger widths of both components as compared with our experiments, 0.7 and 6.3 G, respectively, may be attributed to the higher D atom concentrations achieved in Ref. [28].

The ESR lines of H and D atoms in the Ne:1%HD sample had a structure similar to that in the Ne:1%D$_2$ sample. We observed the ESR line components which can be associated with trapping H and D atoms in either pure HD or Ne environments.

We also observed that a fraction of H and D atoms in Ne:1%D$_2$ and Ne:1% HD samples forming the C1 component recombines upon raising temperature from 0.1 to 0.9–1.3 K. The C1 component was also strongly diminished upon condensing an unsaturated He film into the sample cell. The D atom recombination rates measured at $T = 0.9$ and 1.3 K: $k_r = 4(2) \times 10^{-21}$ cm^3 s^{-1} and $7(4) \times 10^{-21}$ cm^3 s^{-1}, respectively (Table II), strongly exceed those measured for D atoms in bulk solid D$_2$ samples, $k_r \simeq 10^{-28}$ cm^3 s^{-1} [23], where recombination at these temperatures proceeds on the time scale of hours and days [23]. Similar to the above results, we did not observe recombination of H atoms in bulk HD at $T = 0.13$–1.3 K [23]. We can estimate an upper limit for the recombination rate of H atoms in bulk HD in this temperature range as 3×10^{-25} cm^3 s^{-1} by comparing it to the D atom signal decay due to isotopic exchange reaction D+HD $\rightarrow$ D$_2$+H which rate, 3×10^{-27} cm^3 s^{-1}, was measured in Ref. [23]. The recombination rates of H and D atoms in H$_2$, HD, and D$_2$ clusters turned out to be comparable as presented in Table II. The H and D atoms diffusion in the bulk molecular hydrogen solids is governed by tunneling and a strong dependence of the recombination rate on atomic mass should be expected.

Therefore, we suggest that the recombination of D and H atoms occurs in the clusters of molecular deuterium and HD formed in the Ne:1%D$_2$ and Ne:1%HD solid mixtures which melt after raising the temperature from 0.1 K to 0.9–1.3 K. The D$_2$ clusters formed in the Ne:1%D$_2$ sample have higher melting temperatures than those of H$_2$ and HD clusters and, as a result, a much smaller fraction of the C1 atoms recombines in the Ne:1%D$_2$ sample as compared with those in Ne:1%HD

and Ne:1%H$_2$ samples assuming that the D$_2$ and HD clusters have the same size distribution.

The recombination rates of H and D atoms embedded in clusters and bulk H$_2$, HD, and D$_2$ samples are summarized in Table II. The recombination rates for H and D atoms in clusters of hydrogen isotopes exceed those for bulk solid samples by 5–7 orders of magnitude at the same temperatures. The H and D atom diffusion in the solid hydrogens at $T < 1$ K proceeds via a repetition of tunneling exchange reactions H+H$_2$ → H$_2$+H, H+HD → HD+H, and D+D$_2$ → D$_2$+D [29]. The rates of these exchange reactions in the *gas phase* [25] at low temperatures provide an upper limit for the recombination rates of H and D atoms in the solid molecular hydrogens. The recombination rates for H and D atoms in the clusters of hydrogen isotopes measured in our work exceed these rates (see Table II) by several orders of magnitude which allows us to conclude that another diffusion mechanism takes over which might be expected in the case of cluster melting.

The influence of a helium film which suppresses accumulation of H and D atoms still requires further investigations. The decrease of the melting temperature for clusters compared to that of bulk materials ($T_m = 16.6$ and 18.7 K, for solid HD and D$_2$, respectively) is closely associated with surface effects playing a crucial role in clusters due to their much higher surface-to-volume ratio [30]. We did not observe accumulation of H and D atoms in the clusters of hydrogen isotopes after condensing helium into the sample cell even after the He film was evacuated from the sample cell. We suggest that a monolayer-thick solid He film could still remain in the sample pores and provide cooling conditions to hydrogen clusters bombarded by electrons released from the sample cell walls in the course of tritium decay. Although such a He film is not superfluid, it may provide better cooling for hydrogen clusters due to a smaller Kapitza resistance for H$_2$/He interfaces compared to that of H$_2$/Ne. As a result, the H$_2$ molecules excited by incident electrons can still relax back to the ground state without being dissociated.

In conclusion, we observed formation of molecular D$_2$ and HD clusters in the Ne:1%D$_2$ and Ne:1%HD samples similar to H$_2$ clusters observed previously in the Ne:1%H$_2$ solid mixture. The H and D atoms trapped in such clusters rapidly recombine upon raising the sample cell temperature from 0.1 K to 0.8–1.3 K. It turned out that the recombination of H and D atoms in the HD clusters formed in the Ne:1%HD sample and D atoms stabilized in the D$_2$ clusters formed in the Ne:1%D$_2$ sample takes place at a temperature higher than that for H atoms in the H$_2$ clusters formed in the Ne:1%H$_2$ sample. In addition to that, we observed a synchronous recombination of H and D atoms in the HD clusters with similar recombination rates. This corroborates our conclusion that the clusters of molecular hydrogen isotopes experience a solid-liquid transition upon raising the temperature from 0.1 to 1.3 K. We also suggest that such clusters do not undergo a superfluid transition and remain in a normal state at the temperatures of our experiment.

[1] V. L. Ginzburg and A. A. Sobyanin, Sov. Phys. JETP Lett. **15**, 242 (1972).

[2] S. M. Apenko, Phys. Rev. B **60**, 3052 (1999).

[3] H. J. Maris, G. M. Seidel, and T. E. Huber, J. Low Temp. Phys. **51**, 471 (1983).

[4] P. Sindzingre, D. M. Ceperley, and M. L. Klein, Phys. Rev. Lett. **67**, 1871 (1991).

[5] S. Grebenev, B. Sartakov, J. P. Toennies, and A. F. Vilesov, Science **289**, 1532 (2000).

[6] K. Kuyanov-Prozument and A. F. Vilesov, Phys. Rev. Lett. **101**, 205301 (2008).

[7] M. Boninsegni, J. Low Temp. Phys. **195**, 51 (2019).

[8] D. Scharf, G. J. Martyna, and M. L. Klein, Chem. Phys. Lett. **197**, 231 (1992).

[9] F. Mezzacapo and M. Boninsegni, Phys. Rev. A **75**, 033201 (2007).

[10] E. L. Knuth, F. Schünemann, and J. P. Toennies, J. Chem. Phys. **102**, 6258 (1995).

[11] U. Albrecht, P. Evers, and P. Leiderer, Surf. Sci. **283**, 419 (1993).

[12] K. Eschenroder, H. Kiefhaber, G. Weiss, and J. Classen, J. Low Temp. Phys. **109**, 163 (1997).

[13] S. Sheludiakov, J. Ahokas, J. Järvinen, L. Lehtonen, S. Vasiliev, Y. A. Dmitriev, D. M. Lee, and V. V. Khmelenko, Phys. Rev. B **97**, 104108 (2018).

[14] S. Sheludiakov, J. Ahokas, O. Vainio, J. Järvinen, D. Zvezdov, S. Vasiliev, V. V. Khmelenko, S. Mao, and D. M. Lee, Rev. Sci. Instrum. **85**, 053902 (2014).

[15] S. Vasilyev, J. Järvinen, E. Tjukanoff, A. Kharitonov, and S. Jaakkola, Rev. Sci. Instrum. **75**, 94 (2004).

[16] S. Sheludiakov, J. Ahokas, J. Järvinen, L. Lehtonen, O. Vainio, S. Vasiliev, D. M. Lee, and V. V. Khmelenko, Phys. Chem. Chem. Phys. **19**, 2834 (2017).

[17] J. Helffrich, M. Maley, M. Krusius, and J. C. Wheatley, J. Low Temp. Phys. **66**, 277 (1987).

[18] W. N. Hardy, M. Morrow, R. Jochemsen, B. W. Statt, P. R. Kubik, R. M. Marsolais, A. J. Berlinsky, and A. Landesman, Phys. Rev. Lett. **45**, 453 (1980).

[19] J. Vanier and C. Audoin, *The quantum physics of atomic frequency standards*, The Quantum Physics of Atomic Frequency Standards No. v. 2 (A. Hilger, Bristol, 1989).

[20] I. F. Silvera and J. T. M. Walraven, in *Progress in Low Temperature Physics*, Vol. 10, edited by D. F. Brewer (Elsevier, 1986), pp. 139–370.

[21] J. Ahokas, O. Vainio, J. Järvinen, V. V. Khmelenko, D. M. Lee, and S. Vasiliev, Phys. Rev. B **79**, 220505(R) (2009).

[22] S. Sheludiakov, J. Ahokas, J. Järvinen, L. Lehtonen, S. Vasiliev, Yu. A. Dmitriev, D. M. Lee, and V. V. Khmelenko, J. Low Temp. Phys. **195**, 365 (2019).

[23] S. Sheludiakov, J. Ahokas, J. Järvinen, D. Zvezdov, L. Lehtonen, O. Vainio, S. Vasiliev, D. M. Lee, and V. V. Khmelenko, Phys. Chem. Chem. Phys. **18**, 29600 (2016).

[24] J. Ahokas, O. Vainio, S. Novotny, J. Järvinen, V. V. Khmelenko, D. M. Lee, and S. Vasiliev, Phys. Rev. B **81**, 104516 (2010).

[25] T. Takayanagi and S. Sato, J. Chem. Phys. **92**, 2862 (1990).

[26] Y. A. Dmitriev, J. Low Temp. Phys. **180**, 284 (2015).

[27] E. P. Bernard, R. E. Boltnev, V. V. Khmelenko, V. Kiryukhin, S. I. Kiselev, and D. M. Lee, Phys. Rev. B **69**, 104201 (2004).

[28] M. Sharnoff and R. V. Pound, Phys. Rev. **132**, 1003 (1963).

[29] T. Kumada, Phys. Rev. B **68**, 052301 (2003).

[30] J. Ross and R. Andres, Surf. Sci. **106**, 11 (1981).